Heliyon 10 (2024) e32526

Contents lists available at ScienceDirect

Heliyon

journal homepage: www.cell.com/heliyon

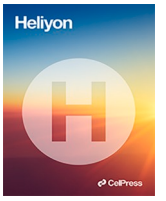

Research article

Study on the molecular mechanisms of Liuwei Dihuang decoction against aging-related cognitive impairment based on network pharmacology and experimental verification

Yin OuYang [a,b], Bowei Chen [b], Jian Yi [b], Siqian Zhou [a,b], Yingfei Liu [a,b], Fengming Tian [a,b], Fanzuo Zeng [a,b], Lan Xiao [c], Baiyan Liu [b,d,*]

[a] The First Clinical College of Traditional Chinese Medicine, Hunan University of Chinese Medicine, Changsha, 410000, China
[b] The First Affiliated Hospital, Hunan University of Chinese Medicine, Changsha, 410000, China
[c] College of Pharmacy, Hunan University of Chinese Medicine, Changsha, 410000, China
[d] Hunan Academy of Chinese Medicine, Changsha, 410000, China

ARTICLE INFO

Keywords:
Liuwei Dihuang decoction
Mild cognitive impairment
Network pharmacology
UPLC-Q-TOF/MS
Experimental validation

ABSTRACT

Objective: Based on network pharmacology and experimental validation, this study aimed to screen the potential targets of Liuwei Dihuang decoction (LW) against mild cognitive impairment (MCI).

Methods: Based on network pharmacology, this study preliminarily explored the targets and molecular mechanisms of LW in the treatment of MCI. The results showed that the mechanism of action of LW against MCI may be related to the cAMP pathway. Then, an aging cell and animal model was established to further verify its molecular mechanism.

Results: A total of 23 active ingredients were identified in LW. In addition, through network pharmacological analysis, we found 22 anti-MCI active ingredients in LW, of which alisol B had the most significant effect, and predicted the potential mechanism pathway by which LW may improve MCI through the cAMP signaling pathway. Further in vivo and in vitro experiments confirmed that LW can alleviate cognitive dysfunction in aging mice and reduce D-galactose-induced senescent cells, which may be through activation of the cAMP/PKA/CREB signaling pathway.

Conclusion: This study found that the traditional Chinese medicine formula LW may play a role in improving MCI by regulating the cAMP/PKA/CREB signaling pathway, which provides a reference for further clinical research on the anti-MCI effect of LW and its molecular mechanism.

1. Introduction

Diseases that cause cognitive impairment have had a significant negative impact on the quality of life for the elderly as the world's population ages. Between normal aging and the dementia transition period, mild cognitive impairment (MCI) is the gradual loss of memory and other cognitive abilities but does not hinder everyday functioning [1]. Memory loss, especially recent memory impairment, is the predominant symptom of MCI. Additionally, MCI sufferers may struggle with attention and executive function issues,

* Corresponding author. The First Affiliated Hospital, Hunan Academy of Chinese Medicine, Changsha, 410000, China.
E-mail address: liubaiyan9657@163.com (B. Liu).

https://doi.org/10.1016/j.heliyon.2024.e32526
Received 12 October 2023; Received in revised form 4 June 2024; Accepted 5 June 2024
Available online 6 June 2024

which include a weakened capacity for organization, planning, and concentration [2]. MCI is one of the risk factors for individuals to develop dementia even if it is not dementia in and of itself. According to studies, MCI is typically common and gradually becomes more common as people age. Every year, between 15 and 20 % of MCI individuals develop dementia. As a result, MCI has recently been recognized as a crucial window for the early diagnosis and management of dementia [3,4].

In my nation, a traditional Chinese medicine(TCM) formulation known as Liuwei Dihuang Decoction (LW) is made up of six medicinal ingredients cooked Radix rehmanniae, Cornus officinalis, Poria cocos, Alismatis, Rhizoma Dioscoreae, and Paeoniaceae. Modern pharmacology has demonstrated that LW possesses antiaging and immune-boosting properties [5]. According to studies, LW has neuroprotective properties, improves cerebral blood flow, reduces oxidative stress, and regulates lipid metabolism, all of which may help improve cognitive dysfunction [6,7]. Relevant clinical investigations have also revealed that the LW may have certain advantages for some MCI patients and may enhance cognitive abilities in MCI patients, including memory and concentration. However, the way in which it treats cognitive impairment caused by aging is still a matter of debate. This merits further investigation.

Network pharmacology is a field of study that examines intricate relationships between medications and biological systems using methods from systems biology, network science, and computational biology. It is based on systems-level knowledge and strives to shed light on pharmacological targets, drug side effects, and drug-disease connections as well as the human body's mechanism of action [8]. To obtain a thorough understanding of the mechanism and impact of medications, network pharmacology conducts systematic investigations on the interaction of pharmacology with numerous targets, numerous pathways, and biological entire systems. To further illuminate the entire impacts and mechanisms of action of TCM, network pharmacology is also utilized in the formulation and multitarget mode of TCM chemicals and natural products.

Therefore, this study employed network pharmacology and molecular docking to anticipate common targets and candidate compounds for LW treatment of MCI. It also used the ultrahigh performance liquid phase-quadrupole time-of-flight mass spectrometer (UPLC-TOF/MS) method to investigate the active ingredients of LW. Then, using in vitro and in vivo experimental validation, we were able to pinpoint possible targets and offer some theoretical justification for the clinical application of LW for the treatment of MCI.

2. Materials and methods

2.1. Preparation of Liuwei Dihuang decoction

Radix rehmanniae, Cornus officinalis, Poria cocos, Alismatis, Rhizoma Dioscoreae, and Paeoniaceae are all cooked for LW (Table 1). The decoction pieces were acquired from the First Affiliated Hospital of Hunan University of Traditional Chinese Medicine and were certified as meeting the national pharmacopeia standard by Associate Researcher Hongping Long of the First Affiliated Hospital of Hunan University of Traditional Chinese Medicine.

According to the ratio of medicinal materials of LW, weigh twice the prescribed number of medicinal materials, add them to a 1000 mL round-bottom flask along with five times as much distilled water, soak for 1 h, then heat and boil, condense, and reflux for 1 h, cool, and filter through three layers of gauze. The distilled water was added three times, heated to a boil, condensed and refluxed for half an hour, cooled, and then filtered through three layers of gauze. Utilizing a rotary evaporator, combine the water extraction solution twice to obtain 75 mL of concentrate (each mL of which contains 2 g of crude drug). Rats were given stomach administration of the obtained extract.

2.2. Reagents

Vitamin E(Vit-E) (HY–N0683) was purchased from MedChemExpress Company (New Jersey, USA), and D-galactose (G100367) was purchased from the search banner Biochemical Technology Co., Ltd. (Shanghai, China). A cAMP-element response binding protein (CREB) antibody (1220801-AP) and GAPDH antibody(10494-1-AP) were purchased from Proteintech Group, Inc (Wuha, China). Cyclic adenosine phosphate (cAMP) antibody (ab76238), protein kinase A (PKA) antibody(ab75991), and p-CREB antibody(ab32096) were purchased from Abcam (United States). CCK-8(MA0218) was purchased from Dalian Meilun Biotechnology Co., Ltd (Dalian, China). The HRP-sheep anti-rabbit secondary antibody (E-AB-1003) was purchased from Elabscience Biotechnology Co., Ltd(Wuhan, China). The β-galactosidase staining kit(G1580) was purchased from Solaibao Technology Co., Ltd.(Beijing, China).

Table 1
Composition of LW.

Scientific name	English name	Date of manufacture	Batch number	Weight
Rehmannia glutinosa (Gaertn.) DC.	Radix Rehmanniae	2023.04.13	23041333	24 g
Cornus officinalis Siebold & Zucc.	Cornus Officinalis	20230609	HY23052203	12 g
Dioscorea oppositifolia L.	Rhizoma Dioscoreae	20230620	NG23052905	12 g
Paeonia suffruticosa Andr.	Paeoniaceae	20230506	HH23041702	9 g
Alisma orientalis(Sam.)Juzep.	Alismatis	20230610	GW23052902	9 g
Wolfiporia extensa (Peck) Ginns.	Poria Cocos	20230615	NG2305001B	9 g

2.3. Analysis of in vitro components of LW

2.3.1. Sample preparation

Ten milliliters of LW concentrate was transferred to an evaporation dish, a water bath was used to further concentrate, 30 ml of methanol solution was added, and the mixture was sonicated for 30 min (power 250 W, frequency 40 kHz). Centrifuge 2 mL of the supernatant at 3000 r·min^{-1} for 5 min (centrifuge radius: 11 cm). To obtain the test solution, centrifugation should be followed by the supernatant being filtered through a 0.22 μm microporous filter.

2.3.2. Chromatographic and mass spectrometry detection conditions

Chromatographic conditions: The chromatographic column was Agilent ZORBAX Eclipse Plus C18 (3.0 mm × 100 mm, 1.8 μm), the mobile phase was composed of organic phase acetonitrile (A) and aqueous phase (B), and the aqueous phase (B) contained 1 % ammonium formate (mass spectrometry level), layer elution (0–5 min, 5 %–15 % A; 5–10 min, 15 %–35 % A; 10–20 min, 35 %–65 % A; 20–40 min, 65 %–85 % A); flow rate: 0.4 mL · min-1; injection volume: 2 μL.

Mass spectrometry conditions: positive and negative ion analysis mode is used; ionization method is electrospray ionization (ESI); Agilent standard tuner (G1969-85000) is used for accurate mass number correction before injection analysis; first-order mass spectrometry scanning detection range: *m/z* 100–1700; nitrogen is used as solvent removal drying gas; temperature is 325 °C; flow rate is 6.8 L min^{-1}, sheath temperature is 350 °C; capillary voltage is 4.0 kV; fragment voltage is 150 V.

2.4. LW against MCI: network pharmacological analysis

2.4.1. Compile potential LW anti-MCI targets

Based on the 23 LW chemical components identified by UPLC-EISQ-TOF-MS analysis, the target acquisition of these components was performed using the TCMSP database(https://old.tcmsp-e.com/tcmsp.php), PubChem database (https://pubchem.ncbi.nlm.nih.gov/), and SwissTargetPrediction database (http://www.swisstargetprediction.ch/). The term "mild cognitive impairment" was used to search the gene card (https://www.genecards.org/) and OMIM (https://omim.org/) databases for the related target. Through the Venn diagram online mapping website (https://jvenn.toulouse.inrae.fr/app/example.html), the targets of LW active components were compared with the targets of MCI after false positives and duplicate targets were removed in order to identify possible treatment targets.

2.4.2. Construction of the protein-protein interaction (PPI) network

The PPI network between potential treatment targets of LW for MCI was established by selecting "*Homo sapiens*" species from the STRING database (https://string-db.org/).

2.4.3. GO function and KEGG pathway enrichment analysis

The Sangerbox platform (http://sangerbox.com) was used to investigate GO function enrichment and KEGG pathway enrichment. The error incidence rate (FDR) < 0.05 was considerably enriched, and the smaller the FDR was, the higher the significance.

2.4.4. Molecular docking

The 3D structure of the target protein was downloaded from the PDB database and saved in PDB format. Download the 3D structure of the component through the PubChem database and save it in SDF format. Use Open Babel 2.4.1 software was used to convert the SDF format to mol2 or PDB format. It was imported into PyMOL 2.5 to remove water molecules and ligands. The docking module was selected for molecular docking to study the binding activity of the target protein and chemical after importing their processed molecular structures into AutoDock. Finally, PyMOL 2.5 was used to visualize the docking result.

2.5. In vitro validation

2.5.1. Cell culture

Pheochromocytoma cells lines (PC12 cells) were purchased from Purnosys Biotech Co., Ltd. (Wuhan, China). PC12 cells were cultured at 37 °C in a 5 % carbon dioxide incubator using 1640 medium (C11890500, Gibco, New York, USA) supplemented with 10 % fetal bovine serum (10270-106, New York, USA) and 1 % penicillin-streptomycin (SV30010, HyClone, Logan, Utah, USA) [9].

2.5.2. Preparation of blank serum and drug-containing serum

Twenty 2-month-old specific pathogen-free (SPF-grade) male SD rats weighing 220 ± 10 g, were purchased from Hunan Slac Jingda Laboratory Animal Co., Ltd., Changsha, China (license No. SCXK (Xiang) 2019–0004). The experiment was approved by the Ethics Committee for Experiments with Animals of the First Subsidiary Hospital of the Chinese University of Medicine (ZYFY20210710).

Rats were randomly divided into a drug-containing serum group (LW) and a blank serum group. After 1 week of adaptive feeding, rats in the LW-containing serum group were given a clinically equivalent dose of 3 times (2g·ml·d^{-1}) by gavage according to the transformation of human and animal body surface areas. The blank serum group was given the same amount of normal saline twice a day for 5 consecutive days [10]. Two hours after the last gavage, the rats were anesthetized with 3 % sodium pentobarbital at 50 mg/kg, and blood was collected from the abdominal aorta. 1500r·min^{-1} was centrifuged at 4 °C for 10 min, and 56 °C was inactivated

for 30 min and then frozen at −80 °C.

2.5.3. Establishment of the PC12 cell aging model

According to literature reports [11], D-galactose (D-gal) was used to induce PC12 cells to construct an aging model. PC12 cells(1×10^5 cells/mL)were seeded in 96-well plates, and 100 μL of cell suspension was added to each well. After the cells adhered to the wall, different concentrations of D-gal (20, 40, 60, 65, 75 and 80 mg/ml) were added to each well. After 6 h, 12 h, and 24 h, cell viability was determined the appropriate D-gal concentration and time for inducing aging.

2.5.4. Cell viability assay

The effect of drug-containing serum on the viability of PC12 cells was detected by CCK-8 assay. PC12 cells (1×10^5 cells/mL) were seeded in 96-well plates, and 100 μL of cell suspension was added to each well. After the cells adhered to the wall, the cell-based medium was supplemented with different concentrations of drug-containing serum, and the serum concentrations were set to 2.5 %, 5 %, 10 %, 15 %, and 20 %. The control group was cultured in 1640 medium (10 % fetal bovine serum), and each group had 6 replicate wells. After 24 h, CCK-8 solution was added to calculate the biological activity test of drug-containing serum on cells by measuring the absorbance optical density (OD) value.

The effect of LW on the viability of PC12 cells was detected by CCK-8 assay. PC12 cells (1×10^5 cells/mL) were seeded in 96-well plates, and 100 μL of cell suspension was added to each well. After the cells adhered to the wall, the model group was given D-gal, the LW group was given D-gal + drug-containing serum at the same time, and the positive control group was given D-gal + Vit-E (50 μg/ml) [12]. After 12 h of treatment, the CCK-8 solution was added, and the cell viability was determined by measuring the OD value. The above 450 nm wavelength was detected on an enzyme microscope. Inhibition rate (%) = (control group OD value-administration group OD value)/(control group OD value-blank hole OD value) × 100 %.

2.5.5. β-Galactosidase staining

PC12 cells (1×10^5 cells/mL) were seeded in a 24-well plate, and 800 μL of cell suspension was added to each well. After the cells adhered to the wall, the model group was given D-gal, the LW group was given D-gal + LW-containing serum at the same time, the positive drug group was given D-gal + Vit-E, and the control group was given FBS (10 % fetal bovine serum). After 12 h of dosing, the cells were washed once with phosphate-buffered saline (PBS), 1 ml of β-Gal fixative solution was added to each well, and the cells were incubated at room temperature for 15 min. Then, the cells were washed 3 times with PBS, 1 ml of staining solution was added to each well, incubated overnight at 37 °C, and observed and photographed with a normal light microscope. Senescent cells were dyed blue, and the percentage of senescent cells was calculated by ImageJ.

2.5.6. Real-time PCR (RT-qPCR) detection

RT-q PCR was used to detect the mRNA levels of cAMP, PKA and CREB. Total RNA was extracted from PC12 cells using TRIzol reagent according to the instructions. Then, the total mRNA was used as a template for reverse transcription with cDNA reverse transcriptase. The RT-q PCR amplification process was as follows: 95 °C for 1min, 95 °C for 20s, 60 °C for 1min, 40 cycles, melting curve analysis: 60–95 °C. β-actin was selected as the internal reference, and the relative gene expression was calculated with $2^{-\Delta\Delta Ct}$. The primer sequences are shown in Table 2.

2.5.7. Western blot analysis

The total protein of PC12 cells was extracted after lysis and centrifugation, and the protein expression levels of cAMP, PKA, CREB and p-CREB were detected by Western blot. SDS-PAGE, membrane transfer, and sealing were used. The primary antibody was added and incubated at 4 °C overnight. The secondary antibody was added and incubated at room temperature for 1 h the next day and developed by chemiluminescence. The relative protein expression level was calculated by ImageJ.

2.6. In vivo validation

2.6.1. Animals

Sixty 2-month-old SPF grade male C57BL/6 mice, weighing 18–22 g, were purchased from Hunan Slack Jingda Experimental Animal Co., Ltd., with the license number SCXK (Hunan) 2019-0004. This experiment was approved by the Experimental Animal

Table 2
PCR primer sequences of each gene.

Gene name	Primer sequence (5'~3')	Product length
β-actin	F : GCAGATGTGGATCAGCAAGC R : AGGGTGTAAAACGCAGCTCAG	70
PKA	F : TGGACAAGCAGAAGGTGGTG R : TCCCGGTAGATGAGGTCCAG	277
cAMP	F : GGGATGAGGACCCAGATA R : GGCACATTGCTCAGGTAA	95
CREB	F : CTGGATGACCCCATGGACCT R : AGAAGCCGAGTGTTGGTGACTA	236

Ethics Committee of the First Affiliated Hospital of Hunan University of Traditional Chinese Medicine (ZYFY20210710).

2.6.2. Experimental program

60 mice were randomly divided into 5 groups after adaptive feeding for 7 days：control group, model group, Vit-E(200 mg kg^{-1}) group, low-dose LW (LW-L) (10 g kg^{-1}) group and high-dose LW (LW-H) (20 g kg^{-1}). Except for mice in the control group, mice in other groups were injected subcutaneously with 100 mg kg^{-1} D-gal [13] once a day for six weeks. Subcutaneous injection of D-gal is a common method for replicating aging models [14]. The mice in the control group were injected with an equal amount of normal saline. After conducting the Morris water maze (MWM) test on the 6th week, we anesthetized all mice by intraperitoneal injection of 1 % sodium pentobarbital. Collect mouse hippocampi and place them on ice. All samples were stored at −80 °C until further use.

2.6.3. Morris water maze test

The MWM is used to detect the learning and memory abilities and cognitive functions of mice. According to previous reports [15], a black circular pool (depth 60 cm, used diameter 120 cm), the platform is fixed in the second quadrant, tap water is added to the pool, the water level is 1 cm above the platform, the water temperature is controlled at 22–24 °C. Record the time it takes for the mouse to find the submerged platform. If the platform is found within 60 s, the animal is allowed to stay on the platform for 5 s; if the platform is not found, the animal is guided to the platform for 5 s. Each animal was trained four times per day, with 15–20 min between sessions, for 5 days. A video tracking system records the animal's location, swimming distance and time. On the sixth day, the platform was dismantled, and the animals were put into the water starting from the other side of the original platform quadrant. The latency and number of times the animals crossed the original platform quadrant within 60 s were recorded.

2.6.4. Nissl stain

After the mice were anesthetized, the brains were harvested after cardiac perfusion. After being fixed in 4 % paraformaldehyde for 48 h, they were embedded in paraffin, coronally sectioned, and Nissl staining was performed to evaluate neuronal damage in the hippocampal region of the brain tissue.

2.6.5. Real-time PCR (RT-qPCR) detection

RT-q PCR was used to detect the mRNA levels of cAMP, PKA and CREB. Total RNA was extracted from brain tissue using TRIzol reagent according to the instructions. Then, the total mRNA was used as a template for reverse transcription with cDNA reverse transcriptase. The RT-q PCR amplification process was as follows: 95 °C for 1min, 95 °C for 20s, 60 °C for 1min, 40 cycles, melting curve analysis: 60–95 °C. β-actin was selected as the internal reference, and the relative gene expression was calculated with $2^{-\Delta\Delta Ct}$. The primer sequences are shown in Table 3.

2.7. Statistical analysis

SPSS 21.0 software (SPSS INC., Chicago, USA) was used for statistical analysis. The measurement data conforming to the normal distribution were expressed as $\bar{\chi} \pm s$, and a one-way analysis of variance was used to compare the mean between multiple groups, the least significant difference(LSD) test for multiple comparisons. $P < 0.05$ indicated that the difference was statistically significant.

3. Results

3.1. Analysis of chemical constituents of LW

Twenty-three useful components from the LW extract were examined using UPLC-QTOF-MS detection, accurate relative molecular mass, mass-to-charge ratio, and other mass spectrometry information combined with reference comparison, consulting pertinent literature. Among them, 23 components such as morroniside, loganin, and paeonol, are shown in Table 4.

Table 3
PCR primer sequences of each gene.

Gene name	Primer sequence (5'~3')	Product length
β-actin	F：GCAGATGTGGATCAGCAAGC	70
	R：AGGGTGTAAAACGCAGCTCAG	
PKA	F：CAACAACCGAGTGTGCTTGAT	87
	R：TCATTTGCGATCCGAGTCTGG	
cAMP	F：TGGCGGTCACTATCACTG	250
	R：AGGCACATTGCTCAGGTAG	
CREB	F：GCAACCACACTTAACCGAATTACCG	144
	R：CTGGCTGTCCTGGAACTCACTTATG	

Table 4
Analysis of components of LW.

Number	RT	Positive Ion Mode	Negative Ion Mode	Molecular Mass	Molecular Formula	Name	Deviation (ppm)
1	2.085	M + H 127.0376	/	126.0304	$C_6H_6O_3$	5-hydroxymethylfurfural	(+) 11.96
2	6.988	M + Na 399.1252	M − H 375.1301	376.36	$C_{16}H_{24}O_{10}$	Loganic acid	(+) 4.01 (−) −1.05
3	7.616	M + Na 429.1270	M + COOH 451.1462	406.3817	$C_{17}H_{26}O_{11}$	Morroniside	(+) 0.68
4	8.383	M + H 497.0945	M − H 495.1513	496	$C_{23}H_{28}O_{12}$	Oxypaeoniflora	(+) −4.15 (−) −0.83
5	10.393	M + H 483.1462	M − H 481.1114	482.1392	$C_{31}H_{46}O_4$	Polyporenic acid C	(+) −1.51
6	10.614	M + Na 413.1369	M + COOH 435.1513	390.38	$C_{17}H_{26}O_{10}$	Loganin	(+) 2.75
7	12.387	M + Na 503.1504	M + COOH 525.162	480.45	$C_{23}H_{28}O_{11}$	Paeoniflorin	(+) 4.34
8	14.374	M + H 447.1272	M + COOH 491.1198	446.404	$C_{22}H_{22}O_{10}$	Syringaresino	(+) 3.07
9	17.275	M + H 397.304	/	396.2948	$C_{28}H_{44}O$	Ergosterol	/
10	18.543	M + NH_4 618.2174	M − H 599.1769	600.1843	$C_{30}H_{32}NO_{13}$	Benzoyloxypaeoniflorin	(+) 0.98 (−) 0.42
11	19.149	M + NH_4 618.2181	M − H 599.1780	600.57	$C_{30}H_{35}NO_{13}$	Mudanpioside C	(+) 0.47 (−) −1.47
12	20.105	M + H 285.0747	M − H 283.0618	284.0684	$C_{16}H_{12}O_5$	Calycosin	(+) 3.1 (−) −2.06
13	21.336	M + NH_4 602.2216	M + COOH 629.1885	584.57	$C_{30}H_{35}NO_{12}$	Benzoylpaeoniflorin	(+) 3.04
14	23.886	M + H 167.0698	M − H 164.8361	166.18	$C_9H_{10}O_3$	Paeonol	(+) 2.39
15	24.668	M + H 269.0799	M − H 267.0664	268.0736	$C_{10}H_{13}N_5O_4$	Adenosine	(+) 3.07 (−) −0.59
16	24.849	N + H 529.3506	M + COOH + H2O 591.3536	528.3435	$C_{32}H_{48}O_6$	Alisol C 23-acetate	(+) 2.96
17	26.292	N + H 529.3508	M − H 527.3377	528.3438	$C_{33}H_{52}O_5$	Pachymic acid	(+) 2.57
18	26.514	M + NH_4 274.2749	/	256.42	$C_{16}H_{35}NO_2$	Palmitic acid	(+) −1.98
19	28.563	M + H 487.3402	M − H 485.3273	486.693	$C_{30}H_{46}O_5$	Alisol C	(+) 3.26
20	30.843	M + NH_4 302.3033	/	284.48	$C_{18}H_{39}NO_2$	stearic acid	(+) 6.16
21	33.229	M + H 473.3606	/	472.3535	$C_{30}H_{48}O_4$	Alisol B	(+) −4.67
22	33.948	M + Na 555.3643	M + COOH 577.3749	532.762	$C_{32}H_{48}O_4$	Alisol A,24-acetate	(+) 2.49
23	35.754	M + H 515.3713	M + COOH + H2O 577.3742	514.74	$C_{32}H_{50}O_5$	Alisol B 23-acetate	(+) 2.92

3.2. Network pharmacology study of anti-MCI of LW active ingredients based on UPLC-Q-TOF-MS analysis

3.2.1. Prediction of Anti-MCI core targets of LW

The TCMSP and SwissTarget prediction databases were used to collect 23 targets of LW compounds, and 315 possible LW targets were identified. At the same time, a total of 3227 MCI targets were obtained. After matching the potential targets of LW with the potential targets of MCI using the Venn diagram online drawing website, a total of 218 anti-MCI targets of LW were identified (Fig. 1A).

The LW's effective ingredient-target network diagram was created using Cytoscape 3.9.2. The diagram (Fig. 1B) included 239 nodes and 548 edges. The Network Analyzer in the software is used to determine the degree analysis, and the greater the degree value of the nodes, the more edges connected to them. Paeoniflorin, morroniside and loganin are some of the substances with higher degree values in the network diagram. Alisol B is one of them and has 55 interaction targets. LW's essential ingredients for preventing and treating MCI may be those with the most targets.

The STRING database was used to import the 218 common targets to create the PPI network. The network's nodes without connections were set to conceal, the lowest interaction score was set to "the highest confidence level (0.900)," and all other parameters were left at their default settings.

For visualization and analysis, the acquired data were downloaded in TSV format and put into Cytoscape 3.9.2 software (Fig. 1C). The degree value of the node is represented by the node area. With nodes such as VEGFA, GAPDH, AKT1, EGFR, SRC, etc., the greater the node area, the deeper the color, and the higher the matching degree value, indicating that the node is more significant.

3.2.2. GO function and KEGG pathway enrichment analysis

The core targets were entered into the Sangerbox platform database, the analyzed organisms were selected as *Homo sapiens*, GO function enrichment and KEGG pathway enrichment analysis were performed, and the top 10 FDRs were sorted from small to large to draw GO function enrichment bubble maps (cell components, molecular functions, biological processes), and KEGG pathway enrichment bubble maps.

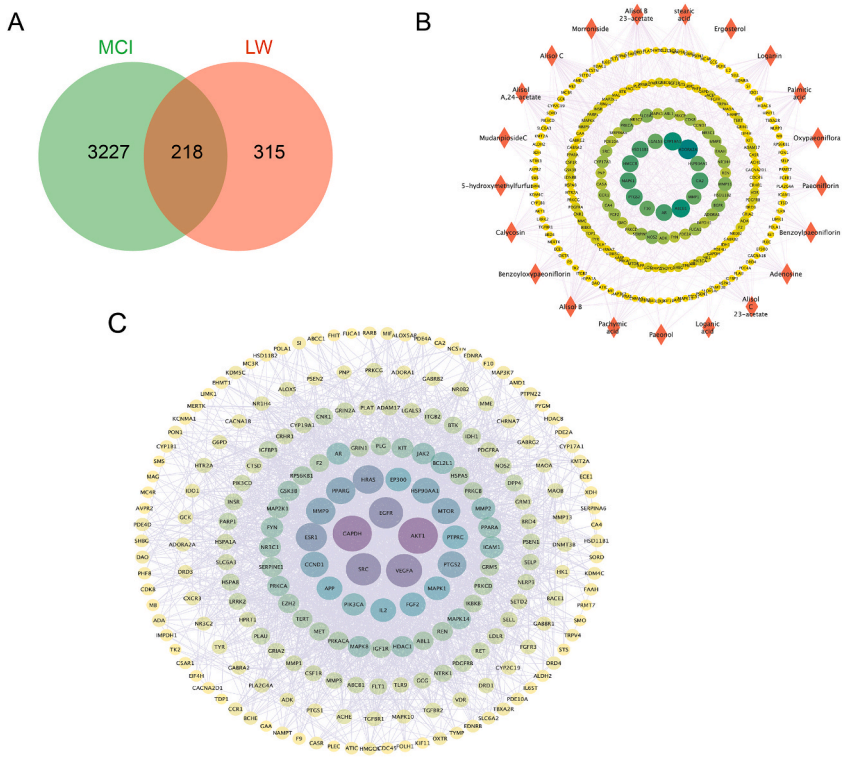

Fig. 1. Core target of LW against MCI. **(A)** LW-MCI Venn diagram. **(B)** LW active ingredient-target diagram. **(C)** PPI network diagram.

GO function results show that the biological processes related to the pathogenesis of MCI are mainly involved in protein phosphorylation, cellular response to amyloid-beta, cytokine-mediated signaling pathways, etc. The cellular components related to the pathogenesis of MCI mainly involve the plasma membrane, membrane raft, neuronal cell body, perinuclear region of cytoplasm, etc. In addition, there are molecular functions related to the pathogenesis of MCI mainly involve ATP binding, protein tyrosine kinase activity, protein serine/threonine kinase activity, endopeptidase activity, etc. (Fig. 2A and B).

KEGG pathway enrichment analysis of core targets showed that the pathogenesis of MCI mainly involves Ras, PI3K-Akt, cAMP, HIF-1, MAPK signaling pathway, etc. (Fig. 2C).

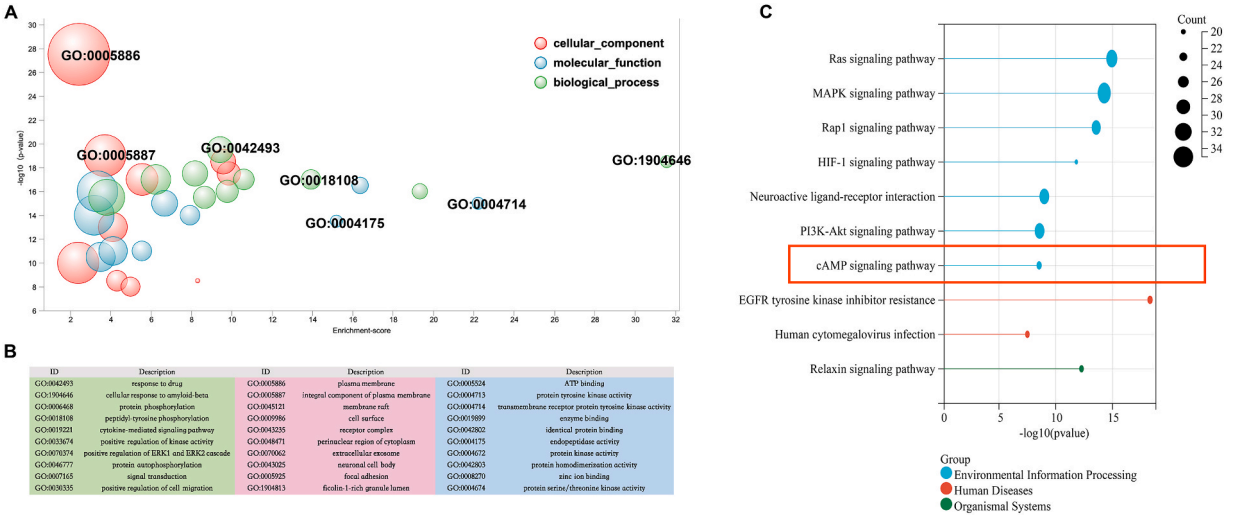

Fig. 2. GO function analysis and KEGG enrichment analysis. **(A)** GO function analysis abundance bubble map. **(B)**GO function analysis table. **(C)** KEGG enrichment analysis map.

3.2.3. Constructing the component-target-pathway network

According to the results of the KEGG pathway enrichment analysis, an active ingredient-target-pathway network diagram (Fig. 3) was constructed, with 147 nodes and 737 edges. The targets involved in the top 10 pathways were MAPK1, PPARG, AKT1, MMP8, etc. The main active ingredients binding to the top 10 pathways were benzoylpaeoniflorin, alisol B, alisol C, pachymic acid, etc.

3.2.4. Molecular docking

Through relevant literature reports, it has been found that the mechanism of action for the prevention and treatment of MCI may be related to the cAMP pathway [16]. Molecular docking was performed between the top 10 components in LW and the three targets related to the cAMP cell pathway (MAPK1, PPARG, AKT1). A binding energy < -5.0 kJ/mol indicates strong affinity activity. Our results showed that the binding energy of alisol B and benzoylpaeoniflorin to the core target was less than -5.0 kJ/mol, indicating that the active components of LW have good affinity with the targets related to the cAMP pathway, suggesting that LW may play a role in improving MCI by regulating the cAMP pathway (Fig. 4A and B).

3.3. In vitro experimental verification

3.3.1. LW ameliorates D-gal-induced injury of PC12 aging cells

The biological activity of the drug-containing serum on PC12 cells was studied by the CCK-8 assay. The results showed that compared with FBS, the drug-containing serum containing 2.5 %, 5 %, 15 %, and 20 % caused different degrees of damage to the cells ($P < 0.001$), and 10 % of the drug-containing serum had no significant inhibitory effect on PC12 cells (Fig. 5A). Therefore, drug-containing serum at a 10 % concentration was used in subsequent experiments.

To explore the optimal time point for modeling and the concentration of D-gal administration, different concentrations of D-gal were used to detect the viability of PC12 cells at 6 h, 12 h and 24 h after administration. The results showed that with increasing D-gal concentration, the cell inhibition rate increased, indicating that D-gal induced cell aging showed a concentration-dependent trend; after 60 mg/ml D-gal induced PC12 cells for 12 h, the cell inhibition rate reached 50 %, so subsequent experimental modeling used 60 mg/ml D-gal to induce PC12 cells for 12 h (Fig. 5B).

The CCK-8 assay was used to determine that after D-gal intervention, cell viability was significantly reduced. Compared with the Model group, the LW group and the Vit-E group had significantly improved cell viability ($P < 0.001$) (Fig. 5C). Further β-Galactosidase staining also showed that after D-gal intervention, PC12 cells were significantly reduced, morphological shrinkage changed, and more

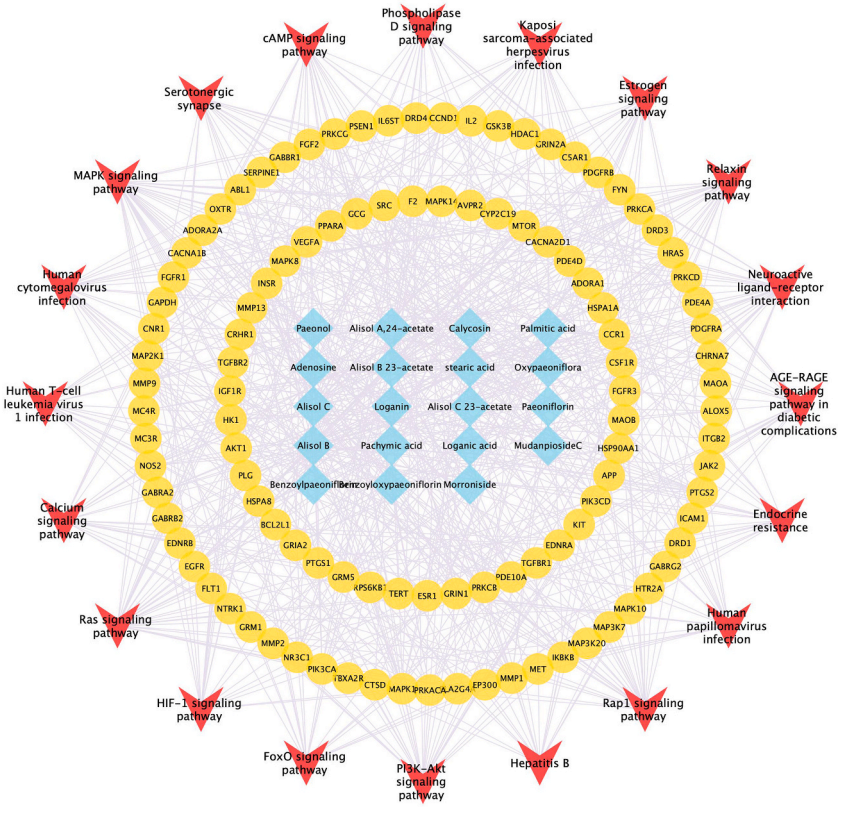

Fig. 3. Component-target-pathway network.

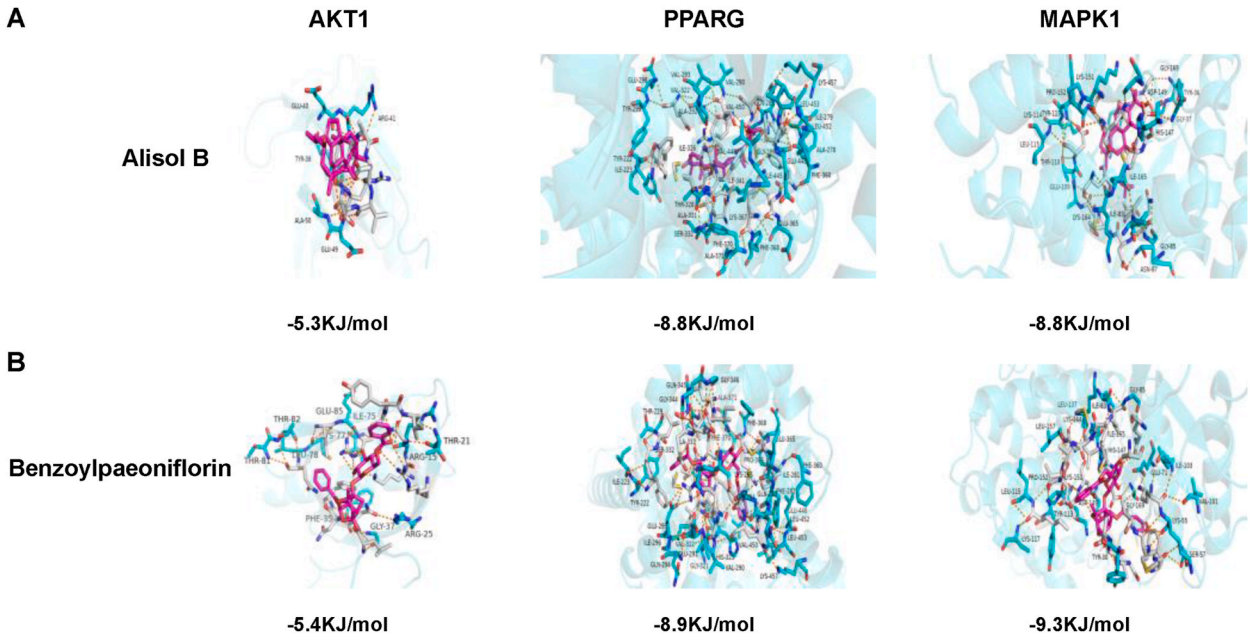

Fig. 4. Binding model of core components and targets of LW. **(A)** Alisol B binding model with core targets. **(B)** Benzoylpaeoniflorin binding model with core targets.

than 40 % of the cells were positive. An aging model was established, while the positive rates of the LW group and the Vit-E group were significantly lower than those of the Model group ($P < 0.001$) (Fig. 5D).

3.3.2. LW increases the mRNA and protein expression of cAMP, PKA and CREB

To further explore whether the drug effect is related to the activation of cAMP/PKA/CREB, the mRNA and protein levels of cAMP, PKA, and CREB were studied in this study. Compared with those in the control group, the cAMP, PKA, and CREB proteins and mRNAs in the model group were significantly reduced ($P < 0.05$ or $P < 0.001$); compared with those in the model group, the mRNA and protein expression levels of cAMP, PKA, and CREB in the LW group and the Vit-E group were significantly increased ($P < 0.05$ or $P < 0.001$) (Fig. 6A–D).

3.4. In vivo experimental verification

3.4.1. Effects of LW on cognitive function in aging mice

During the navigation trials, as training duration and frequency heightened, all groups demonstrated a reduced time to locate the platform. The mice in the control group found the platform faster than those in the model group, with the latter showing significantly increased escape latency ($P < 0.001$). However, the time taken by mice in the treatment groups to find the platform was notably less than that of the model group ($P < 0.001$) (Fig. 7A). Spatial exploration outcomes revealed that, relative to the control group, the model group mice spent a shorter duration in the target quadrant and had fewer platform crossings ($P < 0.001$), suggesting that the cognitive impairments were effectively induced by D-galactose injections. In contrast, mice in both the LW-H and Vit-E treatment groups displayed significantly more time spent in the target quadrant and more platform crossings compared to the model group ($P < 0.001$). Although the LW-L group also showed an increase in these measures, the differences were not statistically significant ($P > 0.05$) (Fig. 7B–D).

3.4.2. Effects of LW on the morphology of hippocampal neurons in aging mice

Relative to the control group, the mice in the model group exhibited significant neuronal damage in the CA1 area, characterized by neuron loss, disrupted organization, cellular atrophy, and edema (Fig. 8A and B). Following treatment with LW or Vit-E, there was a noticeable improvement in neuronal integrity, with the morphology of neurons largely returning to normal and cells being densely and orderly arranged (Fig. 8C–E).

3.4.3. LW increases the mRNA expression of cAMP, PKA and CREB in the brain of aging mice

In comparison to the Control group, levels of cAMP, PKA, and CREB mRNA were significantly lower in the Model group ($P < 0.001$). Relative to the Model group, the expression of cAMP, PKA, and CREB mRNA in both the LW-H and Vit-E groups showed significant elevation ($P < 0.05$). For the LW-L group, there was a notable increase in cAMP and CREB mRNA levels ($P < 0.05$), while the rise in PKA mRNA expression was observed but the difference was not statistically significant ($P > 0.05$) (Fig. 9A–C).

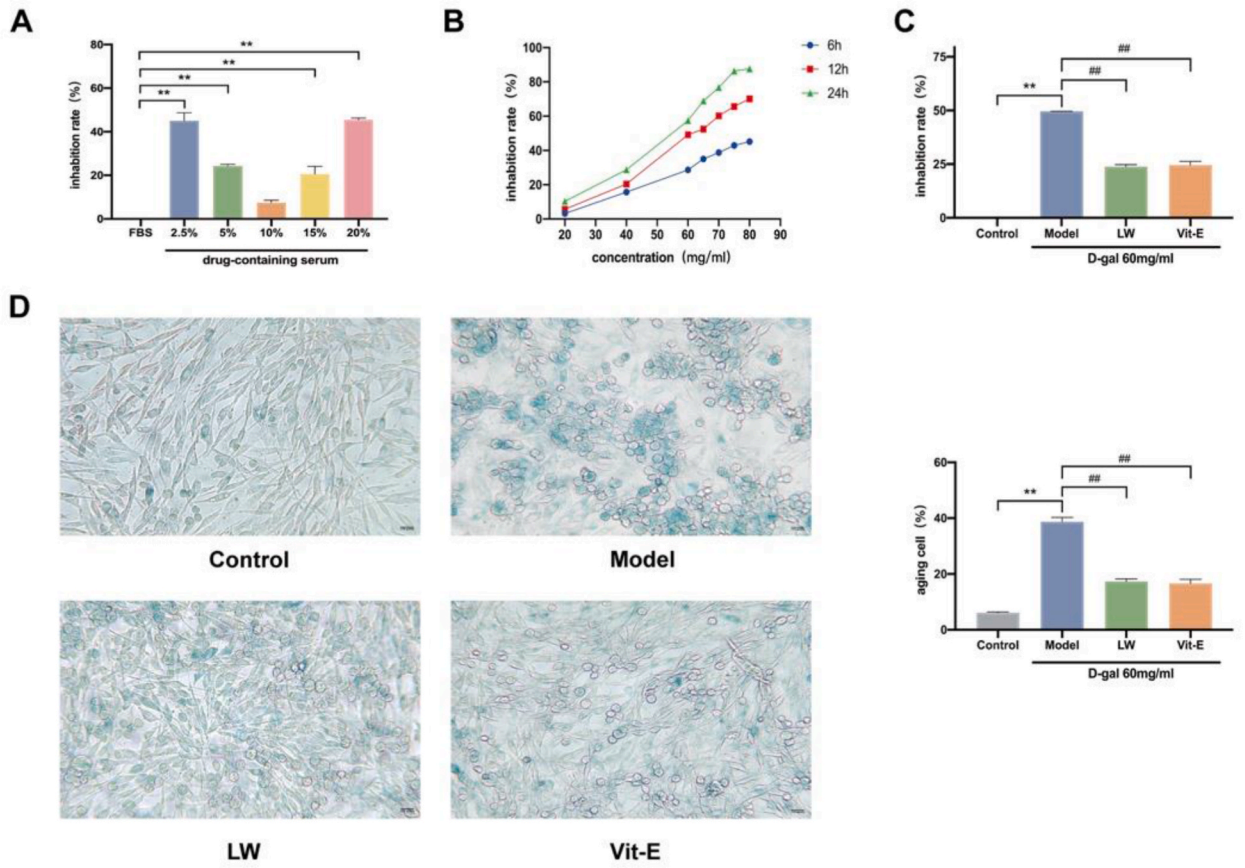

Fig. 5. LW improves the damage to PC12 senescent cells induced by D-gal. **(A)** Validation of drug-containing serum concentration. **(B)** Determining the time point and concentration of D-gal modeling. **(C)** Comparison of the cell inhibition rate after administration. **(D)** β-Galactosidase staining. Compared with the control group, $^{**}P < 0.001$, $^{*}P < 0.05$; compared with the model group, $^{\#\#}P < 0.001$, the difference was statistically significant.

4. Discussion

The prevalence of cognitive impairment is currently high in general. Evaluation and monitoring of cognitive function, alterations to lifestyle, and cognitive training are the main therapy foci for MCI. There is general agreement among experts that people with MCI should have their cognitive decline slowed and their quality of life increased. As a typical medication for renal tonification, LW exhibits the qualities of relative safety and few side effects. LW has been shown by preliminary and related studies of the study team to considerably enhance the cognitive function of aged mice [17,18]. To treat MCI, LW has been considered a possible prescription. However, it has only been demonstrated that it plays a part in a certain pathogenic relationship; further study is still needed to understand the mechanism and screening of active substances in TCM.

In this study, the 23 primary active ingredients of LW—primarily morroniside, loganin, paeonol, etc.—were analyzed using UPLC-Q-TOF-MS technology. LW's anti-MCI targets were developed, and 218 shared targets—targets of VEGFA, GAPDH, AKT1, EGFR, and SRC—were discovered between LW and MCI. The LW against MCI may contain alisol B, paeoniflorin, morroniside and loganin, according to the active ingredient-target network map that was created. Modern pharmacology has demonstrated that Alisol B can control neurotransmitter changes and maintain neurotransmitter balance in the brain [19]. Morroniside acts on the nervous system to promote nerve regeneration and repair, resist oxidative stress, reduce nerve cell apoptosis, inhibit the inflammatory response, and promote cerebral angiogenesis [20]. Loganin has been shown to improve scopolamine-induced learning and memory impairment in mice in more studies [21]. Meanwhile, paeoniflorin has been shown to have neuroprotective, hepatoprotective, and antidepressant effects, as well as the ability to improve cognition and lessen learning disorders and other clinical symptoms of central nervous system (CNS) diseases [22]. This suggests that LW may function as an anti-MCI agent by combining a number of components and numerous targets, in addition to possessing a variety of active substances and having a diversity of pharmacological effects.

Additional network pharmacological investigation revealed that Ras, PI3K-Akt, cAMP, HIF-1, MAPK, and other signaling pathways were among the possible therapeutic targets of LW. According to a review of the literature, blocking the Ras pathway can reduce amyloid buildup in mouse brains and improve cognitive impairment [23]. Relevant studies have demonstrated that the PI3K/AKT and MAPK pathway genes are highly expressed in the brains of dementia patients. The PI3K/AKT pathway can be activated to improve

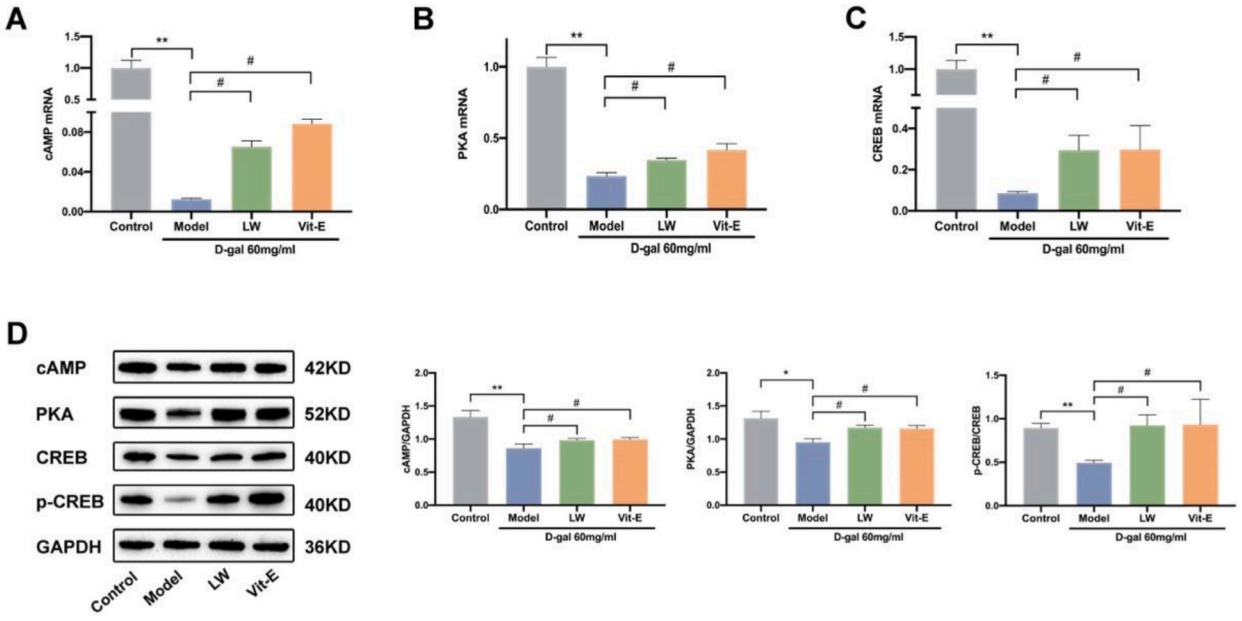

Fig. 6. LW Activates cAMP/PKA/CREB Signaling Pathway. **(A)** Relative expression of cAMP mRNA. **(B)** Relative expression of PKA mRNA. **(C)** Relative expression of CREB mRNA. **(D)** Relative protein expression of cAMP/PKA/CREB. The original images of Western blot are listed in Supplementary Material. Compared with the control group, $^{**}P < 0.001$, $^{*}P < 0.05$; compared with the model group, $^{\#}P < 0.05$, the difference was statistically significant.

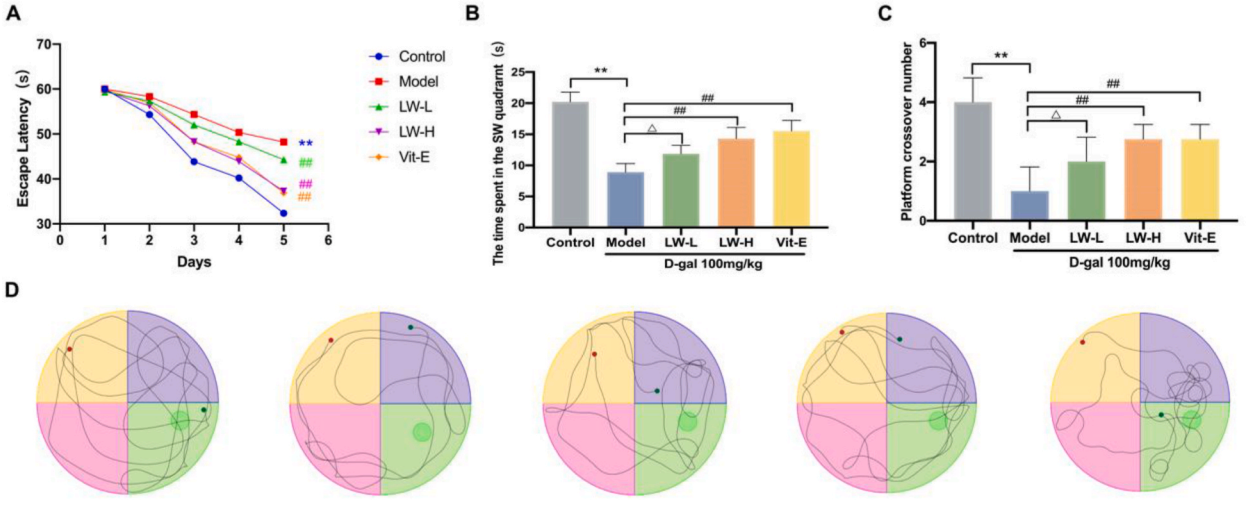

Fig. 7. LW alleviates cognitive dysfunction in aging mice. **(A)** Navigation test. **(B)** Spatial exploration. **(C)** Platform crossing. **(D)** MWM representative figures. Compared with the control group, $^{**}P < 0.001$; compared with the model group, $^{\#\#}P < 0.001$,$^{\#}P < 0.05$, the difference was statistically significant;$^{\triangle}P > 0.05$, the difference was not statistically significant.

cognitive impairment by decreasing lipid peroxidation and inhibiting ferritin autophagy [24,25]. It has been reported that inhibiting the HIF-1 pathway can significantly inhibit the activation of microglia, thereby improving the energy imbalance and metabolic abnormalities of dementia [26]. At the same time, it has been reported that the cAMP signaling pathway plays an important role in MCI, activating the cAMP signaling pathway, thereby inhibiting the expression of cGMP, significantly promoting the formation of synapses in the brain, and improving cognitive dysfunction in mice [27]. At the same time, the molecular docking results showed that the main active ingredients (benzoylpaeoniflorin, alisol B) in LW bound stably with cAMP pathway-related proteins and formed hydrogen bonds.

The cAMP signaling pathway is an important intracellular signaling pathway involved in regulating physiological functions and metabolic processes in cells. In studies related to cognitive dysfunction, abnormal activity of the cAMP pathway has been found to be

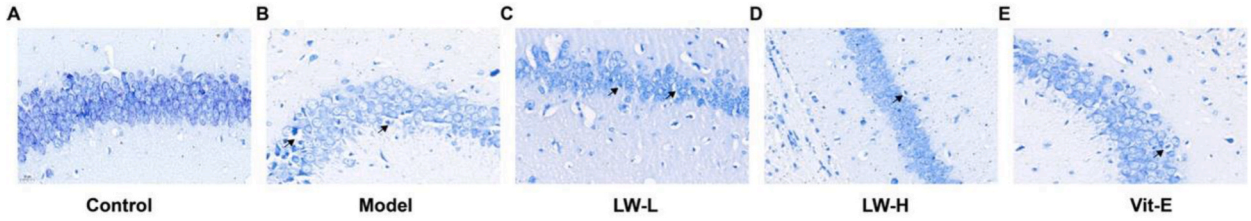

Fig. 8. LW improves hippocampal neuron damage in the brain of aging mice. **(A)**Nissl staining of the hippocampus in the control group. **(B)** Nissl staining of the hippocampus in the model group. **(C)** Nissl staining of the hippocampus in the LW-L group. **(D)** Nissl staining of the hippocampus in the LW-H group. **(E)** Nissl staining of the hippocampus in the Vit-E group.

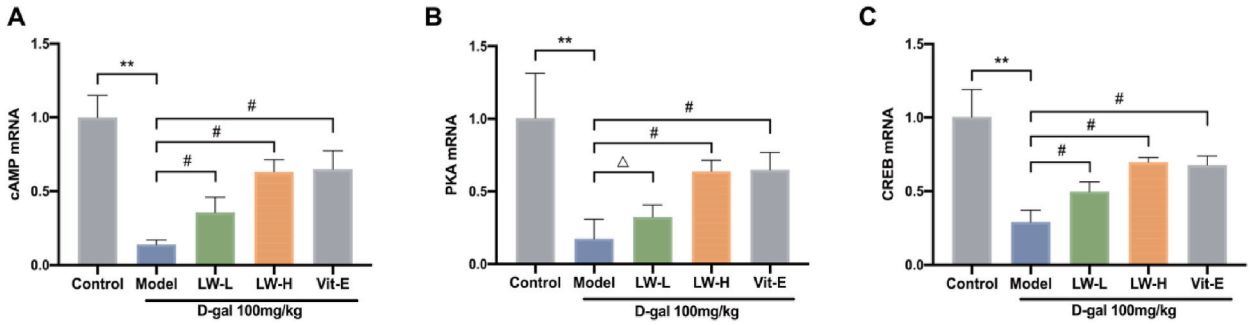

Fig. 9. LW Activates cAMP/PKA/CREB Signaling Pathway. **(A)** Relative expression of cAMP mRNA. **(B)** Relative expression of PKA mRNA. **(C)** Relative expression of CREB mRNA.Compared with the control group, $^{**}P < 0.0001$; compared with the model group, $^{\#}P < 0.05$, the difference was statistically significant.$^{\triangle}P > 0.05$, the difference was not statistically significant.

associated with cognitive impairment and neurodegenerative diseases (such as Alzheimer's disease) [28]. Activation of the cAMP signaling pathway can be achieved through a variety of pathways. One of the key enzymes is adenylyl cyclase, which converts intracellular ATP to cAMP. cAMP further regulates multiple signaling molecules and effector proteins, including protein kinase A (PKA) and cAMP response element binding protein (CREB). Studies have shown that the cAMP pathway may be involved in the protective mechanism of nerve cells and has a certain protective effect on nerve injury and neurodegenerative diseases [29]; it can promote the formation and strengthening of connections between nerve cells, thereby enhancing neuroplasticity [30], and cAMP can regulate presynaptic and postsynaptic signal transduction and affect chemical transmission between nerve cells [31]. This is crucial for information processing and learning and memory processes. Therefore, we speculate that LW may improve cognitive dysfunction by activating the cAMP signaling pathway. Then, in vitro and in vivo experiments confirmed this hypothesis.

The PC12 cell line is the most commonly used cell line in neuroscience research, including studies of neurotoxicity, neuroprotection, neuropsychosis, neuroinflammation, and synaptogenesis. Well-differentiated PC12 cells play a crucial role in the development of neurodegenerative system diseases [32]. In this study, PC12 cells were treated with D-galactose to establish a senescent cell model. Due to the construction of the aging model, the cell morphology changes and shrinks, and the number decreases. After treatment with drug-containing serum, the formation of aging cells can be significantly inhibited. Vitamin E treatment has been shown to delay aging [33]. This study shows that drug-containing serum has the same cellular effect as vitamin E treatment. Further, in vivo experiments confirmed that LW can improve neuronal damage in the brains of aging mice. Relevant studies have demonstrated that activating the cAMP/PKA/CREB signaling system, which is regulated by protein phosphorylation, can alleviate the cognitive impairment caused by aging [34]. This study also demonstrated that LW can increase the relative expression of cAMP, PKA, and CREB mRNA as well as the expression of cAMP, PKA, and p-CREB proteins, indicating that LW has a similar effect to vitamin E and can prevent MCI by activating cAMP/PKA/CREB.

Unfortunately, although in vitro experiments have confirmed that LW can exert anti-MCI effects by activating the cAMP/PKA/CREB signaling pathway, further the specific mechanism by which LW exerts anti-MCI effects is still unknown. Second, although the molecular docking results show that the main components of LW bind well with cAMP pathway-related proteins, it has not been further verified by in vivo and in vitro experiments whether it is the main effective component against MCI. Whether the monomer intervention has a considerable anti-MCI effect is still worth further exploration. Finally, even though we have verified the primary active elements in LW, we have not yet conducted a more thorough analysis of the in vivo components.

5. Conclusion

In conclusion, this research discovered that LW significantly improves cognitive impairment by activating the traditional cAMP/PKA/CREB signaling pathway. The clinical use of LW is greatly impacted by this study, which offers a theoretical foundation for LW to

alleviate cognitive impairment as well as a promising and successful therapeutic strategy for anti-MCI.

Ethics statement

The animal study was reviewed and approved by the Ethics Committee of Laboratory Animal Studies of The First Affiliated Hospital of Hunan University of Chinese Medicine and approved all the experimental protocols (No. ZYFY20210710).

Funding statement

This study was supported by the Youth Program of the National Natural Science Foundation of China (82204924), the Hunan Provincial Natural Science Foundation (2023J30366), the Key Scientific Research Project of Hunan Provincial Department of Education(23A0274) and the Key Program of the Hunan Provincial Administration of Traditional Chinese Medicine (A2023006).

Data availability statement

The data is included in the article.

CRediT authorship contribution statement

Yin OuYang: Writing – review & editing, Writing – original draft, Visualization, Validation, Formal analysis, Data curation. **Bowei Chen:** Writing – review & editing, Resources, Methodology, Investigation. **Jian Yi:** Writing – review & editing, Funding acquisition, Formal analysis. **Siqian Zhou:** Writing – review & editing, Software, Methodology. **Yingfei Liu:** Validation, Conceptualization. **Fengming Tian:** Data curation. **Fanzuo Zeng:** Validation, Conceptualization. **Lan Xiao:** Resources, Funding acquisition. **Baiyan Liu:** Writing – review & editing, Supervision, Project administration.

Declaration of competing interest

We declare that we have no known competing financial interests or personal relationships that could have appeared to influence the work reported in this paper.

Appendix A. Supplementary data

Supplementary data to this article can be found online at https://doi.org/10.1016/j.heliyon.2024.e32526.

References

[1] Lissek Vanessa, Suchan Boris, Preventing dementia? Interventional approaches in mild cognitive impairment, Neurosci. Biobehav. Rev. 122 (2021) 143–164.
[2] H. Kaduszkiewicz, M. Eisele, B. Wiese, et al., Study on aging, cognition, and dementia in primary care patients (AgeCoDe) study group. Prognosis of mild cognitive impairment in general practice: results of the German AgeCoDe study, Ann. Fam. Med. 12 (2) (2014 Mar-Apr) 158–165.
[3] Progression and reversion of mild cognitive Impairment : a study using data from the uniform data set, Chin. General Pract. 25 (9) (2022) 1070–1076.
[4] Gretchen O. Reynolds, Willment Kim, A. Gale Seth, Mindfulness and cognitive training interventions in mild cognitive impairment: impact on cognition and mood, Am. J. Med. 134 (2021) 444–455.
[5] W. Zhou, X. Cheng, Y. Zhang, Effect of Liuwei Dihuang decoction, a traditional Chinese medicinal prescription, on the neuroendocrine immunomodulation network, Pharmacol. Ther. 162 (2016 Jun) 170–178.
[6] J. Wang, X. Lei, Z. Xie, et al., CA-30, an oligosaccharide fraction derived from Liuwei Dihuang decoction, ameliorates cognitive deterioration via the intestinal microbiome in the senescence-accelerated mouse prone 8 strain, Aging (Albany NY) 11 (11) (2019 Jun 3) 3463–3486.
[7] J.H. Wang, X. Lei, X.R. Cheng, et al., A new formula derived from Liuwei Dihuang decoction, ameliorates behavioral and pathological deterioration via modulating the neuroendocrine-immune system in PrP-hAβPPswe/PS1ΔE9 transgenic mice, Alzheimer's Res. Ther. 8 (1) (2016 Dec 13) 57.
[8] C. Nogales, Z.M. Mamdouh, M. List, et al., Network pharmacology: curing causal mechanisms instead of treating symptoms, Trends Pharmacol. Sci. 43 (2) (2022 Feb) 136–150.
[9] Vivek Gautam, Carla D'Avanzo, Oksana Berezovska, et al., Synaptotagmins interact with APP and promote Aβ generation, Mol. Neurodegener. 10 (2015) 31.
[10] Zhe Deng, Zhaoguang Ouyang, Si Mei, et al., Enhancing NKT cell-mediated immunity against hepatocellular carcinoma: role of XYXD in promoting primary bile acid synthesis and improving gut microbiota, J. Ethnopharmacol. 318 (2024) 116945.
[11] Y. Xiao, C. Yang, L. Yu, et al., Human gut-derived B. longum subsp. longum strains protect against aging in a D-galactose-induced aging mouse model, Microbiome 9 (1) (2021 Sep 1) 180.
[12] M. Ye, J. Liu, G. Deng, et al., Protective effects of Dendrobium huoshanense polysaccharide on D-gal induced PC12 cells and aging mice, in vitro and in vivo studies, J. Food Biochem. 46 (12) (2022 Dec) e14496.
[13] Ali, T., Badshah, H., Kim, T., and Kim, M. Melatonin attenuates D-galactose-induced memory impairment, neuroinflammation and neurodegeneration via RAGE/NF-K B/JNK signaling pathway in aging mouse model. J. Pineal Res. 58, 71–85. doi: 10.1111/jpi.12194.
[14] Huang, X., Huang, K., Li, Z., et al. Electroacupuncture improves cognitive deficits and insulin resistance in anOLETF rat model of Al/D-gal induced aging model via the PI3K/Akt signaling pathway. Brain Res. 1740:146834.doi: 10.1016/j.brainres.2020.146834.
[15] S. Hui, Y. Yang, W. Peng, C. Sheng, W. Gong, S. Chen, et al., Protective effects of Bushen Tiansui decoction on hippocampal synapses in a rat model of Alzheimer's disease, Neural Regen. Res. 12 (2017) 1680–1686, https://doi.org/10.4103/1673-5374.217347.
[16] S. Hu, J. Huang, S. Pei, et al., Ganoderma lucidum polysaccharide inhibits UVB-induced melanogenesis by antagonizing cAMP/PKA and ROS/MAPK signaling pathways, J. Cell. Physiol. 234 (5) (2019 May) 7330–7340.

[17] B. Liu, B. Chen, J. Yi, et al., Liuwei Dihuang decoction alleviates cognitive dysfunction in mice with D-galactose-induced aging by regulating lipid metabolism and oxidative stress via the microbiota-gut-brain Axis, Front. Neurosci. 16 (2022 Jul 1) 949298.
[18] W. Xi, N. Song, Q. Yan, et al., The analysis of the effects of Liuwei Dihuang decoction on aging-related metabolites and metabolic pathways in naturally aging mice by ultra-performance liquid chromatography quadruple time-of-light mass spectrometry, J. Physiol. Pharmacol. 72 (3) (2021 Jun).
[19] Q. Ma, L. Han, X. Bi, X. Wang, et al., Structures and biological activities of the triterpenoids and sesquiterpenoids from Alisma orientale, Phytochemistry 131 (2016 Nov) 150–157.
[20] wei Gao, ya Ning, Yujie Peng, et al., Lncrna nkila relieves astrocyte inflammation and neuronal oxidative stress after cerebral ischemia/reperfusion by inhibiting the nf-κb pathway, Mol. Immunol. 139 (2021) 32–41.
[21] Y Cui, Y Wang, D Zhao, Loganin prevents BV-2 microglia cells from Aβ 1-42 1-42 -induced inflammation via regulating TLR4/TRAF6/NF-κB axis, Cell Biol. Int. 42 (12) (2018) 1632–1642, https://doi.org/10.1002/cbin.11060.
[22] Y.X. Zhou, X.H. Gong, H. Zhang, et al., A review on the pharmacokinetics of paeoniflorin and its anti-inflammatory and immunomodulatory effects, Biomed. Pharmacother. 130 (2020 Oct) 110505.
[23] C.E. Evans, J.S. Miners, G. Piva, et al., ACE2 activation protects against cognitive decline and reduces amyloid pathology in the Tg2576 mouse model of Alzheimer's disease, Acta Neuropathol. 139 (3) (2020 Mar) 485–502.
[24] J.S. Park, J. Lee, E.S. Jung, et al., Brain somatic mutations observed in Alzheimer's disease associated with aging and dysregulation of tau phosphorylation, Nat. Commun. 10 (1) (2019 Jul 12) 3090.
[25] A.A. Belaidi, S. Masaldan, A. Southon, et al., Apolipoprotein E potently inhibits ferroptosis by blocking ferritinophagy, Mol. Psychiatr. (2022 Apr 28), https://doi.org/10.1038/s41380-022-01568-w.
[26] M. Gedam, M.M. Comerota, N.E. Propson, et al., Complement C3aR depletion reverses HIF-1α-induced metabolic impairment and enhances microglial response to Aβ pathology, J. Clin. Invest. 133 (12) (2023 Jun 15) e167501.
[27] J. Lu, C. Zhang, J. Lv, et al., Antiallergic drug desloratadine as a selective antagonist of 5HT2A receptor ameliorates pathology of Alzheimer's disease model mice by improving microglial dysfunction, Aging Cell 20 (1) (2021 Jan) e13286.
[28] Y.W. Zhang, S. Liu, X. Zhang, et al., A functional mouse retroposed gene Rps23r1 reduces Alzheimer's beta-amyloid levels and tau phosphorylation, Neuron 64 (3) (2009 Nov 12) 328–340.
[29] R. Ricciarelli, E. Fedele, cAMP, cGMP and amyloid β: three ideal partners for memory formation, Trends Neurosci. 41 (5) (2018 May) 255–266.
[30] A. Roy, M. Jana, M. Kundu, et al., HMG-CoA reductase inhibitors bind to PPARα to upregulate neurotrophin expression in the brain and improve memory in mice, Cell Metabol. 22 (2) (2015 Aug 4) 253–265.
[31] B. Gong, O.V. Vitolo, F. Trinchese, et al., Persistent improvement in synaptic and cognitive functions in an Alzheimer mouse model after rolipram treatment, J. Clin. Invest. 114 (11) (2004 Dec) 1624–1634.
[32] B. Wiatrak, A. Kubis-Kubiak, A. Piwowar, E. Barg, PC12 cell line: cell types, coating of culture vessels, differentiation and other culture conditions, Cells 9 (4) (2020 Apr 14) 958.
[33] R.J. Kryscio, E.L. Abner, A. Caban-Holt, et al., Association of antioxidant supplement use and dementia in the prevention of Alzheimer's disease by vitamin E and selenium trial (PREADViSE), JAMA Neurol. 74 (5) (2017 May 1) 567–573.
[34] J. Lu, C. Zhang, J. Lv, et al., Antiallergic drug desloratadine as a selective antagonist of 5HT2A receptor ameliorates pathology of Alzheimer's disease model mice by improving microglial dysfunction, Aging Cell 20 (1) (2021 Jan) e13286.